Phonon Softening due to Melting of the Ferromagnetic Order in Elemental Iron

Qiang Han,[1] Turan Birol,[2] and Kristjan Haule[1]
[1]Department of Physics and Astronomy, Rutgers University, Piscataway, New Jersey 08854-8019, USA
[2]Department of Chemical Engineering and Materials Science, University of Minnesota, Minneapolis, Minnesota 55455, USA

(Received 19 May 2017; revised manuscript received 3 January 2018; published 4 May 2018)

We study the fundamental question of the lattice dynamics of a metallic ferromagnet in the regime where the static long-range magnetic order is replaced by the fluctuating local moments embedded in a metallic host. We use the *ab initio* density functional theory + embedded dynamical mean-field theory functional approach to address the dynamic stability of iron polymorphs and the phonon softening with an increased temperature. We show that the nonharmonic and inhomogeneous phonon softening measured in iron is a result of the melting of the long-range ferromagnetic order and is unrelated to the first-order structural transition from the bcc to the fcc phase, as is usually assumed. We predict that the bcc structure is dynamically stable at all temperatures at normal pressure and is thermodynamically unstable only between the bcc-α and the bcc-δ phases of iron.

DOI: 10.1103/PhysRevLett.120.187203

The theoretical description of the interplay between structural, magnetic, and electronic degrees of freedom in transition metals at finite temperatures is a central problem of condensed matter physics. The elemental iron is the archetypical system to study the coupling of the ferromagnetism and electronic degrees of freedom with crystal structure, and its importance in both geophysics at high temperatures and high pressures and metallurgy at normal pressure but a finite temperature has made iron one of the most thoroughly studied materials. Its magnetic and mechanical properties undergo major changes through a series of structural phase transitions, but a clear understanding of the feedback effect of magnetism on the structural stability has been elusive.

Elemental iron crystalizes in four different polymorphs; among them are two body-centered cubic (bcc) phases and a face-centered-cubic (fcc) phase, all realized at normal pressure. The bcc-α phase is stable below 1185 K; the fcc-γ phase follows and is stable up to 1670 K, where it is transformed to the bcc-δ phase, which is stable up to the melting point around 1811 K. The α phase is ferromagnetic (FM) below the Curie temperature $T_c = 1043$ K.

Many theoretical methodologies to describe the energetics of magnetic materials, and the stability of different allotropes, have been developed over the past few decades. The conventional density functional theory (DFT), in its generalized gradient approximation (GGA), predicts quite well the magnetic properties of the FM bcc structure with the correct moment and good bulk modulus and quite accurate phonon spectra. However, the GGA severely underestimates the stability of the competing nonmagnetic fcc phase, which is around 300 meV higher in energy than the FM bcc phase and is predicted to be dynamically unstable in its nonmagnetic phase, with many imaginary phonon branches [1]. Similarly, the high-temperature bcc-δ phase is dynamically and thermodynamically unstable within this standard approach.

To simulate the interplay between the lattice dynamics and the presence of magnetic moments at a finite temperature in a metallic environment, several approaches have been developed, which broadly fall into three categories: (i) considering static magnetic configurations within the DFT, but disordered in real space [2–5], (ii) supplementing DFT energetics by some information obtained by an auxiliary Heisenberg model, which is exactly solved by the quantum Monte Carlo method [5,6], (iii) dynamic many-body approaches, such as the dynamical mean-field theory (DMFT), which simulate the dynamics on a single site exactly but neglect the exchange-correlation energy between different iron sites [7–9].

To mimic the presence of local moments within the static DFT, Körmann *et al.* [3] developed a methodology for calculating phonon frequencies at very high temperatures in a real-space large unit cell disordered simulation, by employing space averaging within the constrained spin DFT. This approach is closely related to special quasirandom structure methodology [10]. They showed that, in such a real-space disordered state, both the bcc and fcc structures become dynamically stable and that phonons are considerably softer in this high-temperature state than in a ferromagnetic state. Ikeda *et al.* [2] used the same method to study the pressure dependence of phonon spectra. Körmann *et al.* [5] later extended this method to treat the paramagnetic phase as a function of the temperature using an auxiliary Heisenberg model simulation. It was shown that such an approach can describe reasonably well the temperature-dependent phonon softening measured in experiments [11,12].

A related method, based on large unit cell DFT calculations, was used in Refs. [4,13] to study the pressure and temperature dependence of phonon spectra. In this method, the disorder in atomic positions is coming from thermal vibrations of the lattice rather than from the disorder in spin orientations; hence, it includes anharmonic effects due to the phonon-phonon interaction. It was noticed in Ref. [13] that nonmagnetic disordered state simulations predict both bcc and fcc structures to be dynamically unstable. However, when the simulation is performed in the fictitious long-range antiferromagnetic state, the results are in good agreement with experiments, even when structural disorder is switched off. The inclusion of lattice dynamical effects improved the agreement with experiments slightly, but it is clearly not the main force in stabilizing the high-temperature phases of iron. It was thus shown that the presence of magnetic moments, and their role in lattice energetics, is far more important than the thermal disorder in lattice position.

While the above-described studies based on DFT static simulations but with the inclusion of real-space spin disorder are broadly consistent with experimental measurements, their validity relies on the ergodicity of the quantum metallic system. The local fluctuating magnetic moments are disordered in time rather than space, as their Bragg peaks do not show extra broadening beyond standard thermal disorder; hence, the proper treatment of fluctuating moments has to be dynamic. With the advent of the DMFT and its combination with the DFT, the nature of electrons which are partially itinerant, forming metallic bands in iron, and partly localized, giving rise to Curie-Weiss susceptibility, could finally be simulated from *ab initio* [14].

The energetics of the bcc to fcc transition in iron has been addressed by the DMFT method in Ref. [15] and was later extended to study lattice dynamics in the paramagnetic state of bcc and fcc structures [16], but the lattice dynamics of the ferromagnetic state has not been addressed before. Moreover, the authors of Ref. [17] recently ascribed the previously observed phonon softening at the N point in the Brillouin zone [11,12] to the correlation effects changing with the temperature in the paramagnetic state of the system [17]. They predicted that the paramagnetic bcc structure becomes dynamically unstable between 1.2 and 1.4 times the Curie temperature (close to the α to γ transition in iron) and gets progressively more unstable in most branches as the temperature is increased, so that the bcc-δ phase would require a large phonon-phonon interaction to be dynamically stabilized. Consequently, they conclude that the α-γ transition in iron occurs due to this phonon softening at the N point.

So far, the phonon calculations by the DMFT [16–18] were performed only in the paramagnetic state. On the other hand, the DFT-based methods [2,13] always require some sort of static order; hence, the effects of melting the long-range magnetic order with the temperature, and the impact of partially ordered and disordered local magnetic moments on phonons was not properly addressed before and is the focus of this study. Moreover, previous DFT + DMFT calculations for iron [16,17] were using a nonstationary implementation of DFT + DMFT total energy expression, which is based on the intermediate downfolded auxiliary Hubbard model, and hence the force does not appear as a derivative of a stationary functional. The stationary implementation of the DFT + embedded DMFT functional has recently been achieved [19], and its analytic derivative, which gives rise to the force, was derived in Ref. [20]; hence, the force contains the effects of electronic and magnetic entropy, missing in the previous DMFT approaches. The resulting phonon dynamics, which includes the effects of finite-temperature electronic and magnetic entropic effects, is hence more trustworthy in the high-temperature paramagnetic phases than previous reports.

The physical picture emerging from this state of the art computational technique is very different from previous DMFT reports. (i) The first-order phase transition from the alpha to the gamma phase is unrelated to the observed phonon softening in iron. (ii) The experimentally observed softening of phonons and their nonharmonic change is a consequence of the melting of the long-range ferromagnetic order, and, once the paramagnetic state is reached, the change of the phonons with the temperature is reasonably well explained by the quasiharmonic approximation. (iii) The bcc state remains dynamically stable at all temperatures, even though the fcc state is thermodynamically the stable phase between the α and δ phases. Consequently, the phonon-phonon interaction is not needed to make the high-temperature bcc-δ phase dynamically stable.

In this Letter, we use the stationary version of the DFT + embedded DMFT method [7,21,22], in which the forces are derivatives of the stationary free energy functional with respect to ion displacement [20]. The continuous time quantum Monte Carlo calculation in its rotationally invariant form is used as the impurity solver [23,24]. The screened value of the Coulomb interaction is determined by the constrained local-density approximation (LDA) method resulting in $U = 5.5$ eV and Hund's exchange interaction $J = 0.84$ eV [25], and we used nominal double counting, which was shown to be very close to exact double counting [26]. The DFT part is based on the `Wien2k` package [27], and we use the LDA functional which, when combined with the DMFT, predicts better crystal structures. This is because in the LDA functional both the electronic bandwidth and equilibrium lattice constants consistently show signatures of overbinding and can both be corrected by adding dynamic correlations, while in GGA the bandwidth shows a similar overbinding tendency, while lattice constants many times shows an underbinding tendency; hence, they are harder to simultaneously correct by a higher-order theory. The phonon spectrum is calculated using the direct approach as implemented in the phonopy package [28].

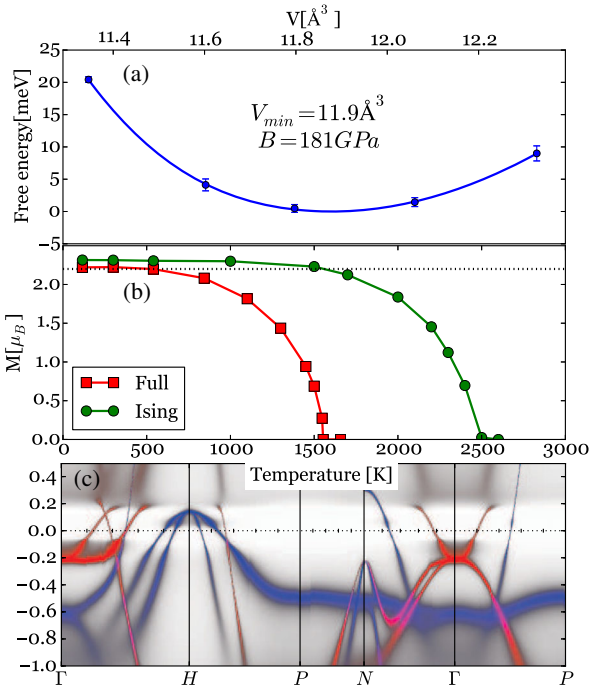

FIG. 1. (a) The electronic free energy per atom versus V of a cubic unit cell. (b) The temperature dependence of the ordered ferromagnetic moment of bcc iron using both the density-density ("Ising") and the rotationally invariant ("full") Coulomb interaction form. (c) The single-particle spectral function of the bcc-α phase at 300 K (the majority and minority spectra are plotted in blue and red, respectively).

In Fig. 1(a), we show the free energy versus the volume of a bcc unit cell at room temperature, which gives the equilibrium volume 11.9 Å^3 and bulk modulus 181 GPa, which are in good agreement with experimental values of 11.69 Å^3 [29] and 172 GPa [1]. Figure 1(b) shows the magnetization versus the temperature curve, which follows the mean-field type of behavior and gives an almost exact magnetic moment 2.2μ_B. The transition temperature ($T_c^{\text{full}} = 1550$ K) in this direct calculation is overestimated, as expected for a method which treats spatial correlations on a mean-field level; consequently, the phase with short-range order is typically predicted to have stable long-range order. We also show the same magnetization curve for the case when the Coulomb interaction is approximated with the density-density terms only (Ising approximation) to demonstrate that such an approach, which was previously used in Refs. [15–17], leads to a much higher transition temperature and a somewhat larger magnetic moment. This effect was also noticed in Refs. [30,31] using the Hirsch-Fye quantum Monte Carlo method but was neglected in previous studies of lattice dynamics. In Fig. 1(c), we also show the electronic spectral function at 300 K, which is in very good agreement with angle-resolved photoemission spectroscopy (ARPES) measurement of Ref. [32] (see Supplemental Material [33] for more detail, which includes additional Refs. [34–64]), in contrast to earlier DMFT calculations based on approximate impurity solvers [65]. We note that a similar magnetization curve for iron was shown in Ref. [14] using a reduced temperature and a reduced moment, but here we show that the same interaction parameters lead to a very precise absolute value of the magnetic moment and the correct equilibrium lattice constant, as well as the correct renormalization of the electronic band structure, as measured by ARPES.

In Fig. 2, we show the phonon spectra calculated in the three bcc phases of iron, in the ferromagnetic state at room temperature, in the paramagnetic α state slightly above the Curie temperature ($1.125T_c$), and in the bcc-δ phase at a high temperature, and we compare it to the measured spectra from Refs. [11,66,67]. They are compared at the same scaled temperature T/T_c in the FM state, as T_c is overestimated in our calculation, while in the paramagnetic state ($T \sim 1800$ K) we use the absolute temperature, because the electronic structure above T_c depends primarily on the lattice constant (which is taken from the experiment). We notice a reasonable agreement between the theory and experiment and a slight deviation around the H point. Notice also that the paramagnetic ($1.125T_c$) solution within the standard DFT has many unstable branches [16], which are here stabilized by a proper description of the fluctuating moments existing above T_c.

Next, we show in Fig. 3(a) the temperature dependence of the theoretically obtained phonon spectra in the bcc phase from a low temperature through the magnetic transition and up to the α-γ transition. We notice a very strong softening of the lowest branch at the N point, which

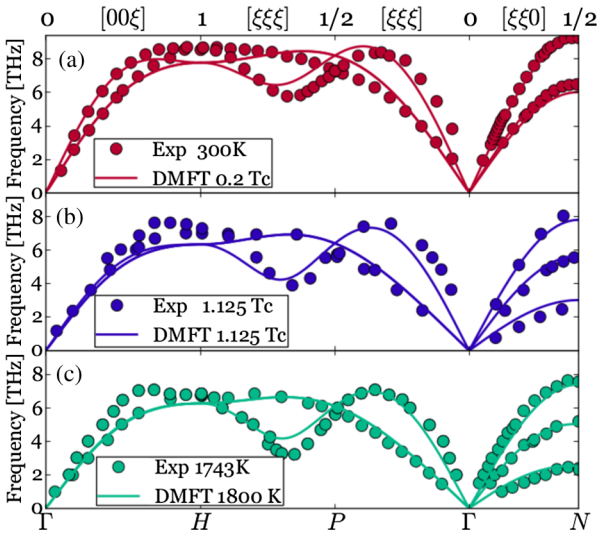

FIG. 2. Phonon spectrum at a low temperature ($T = 300$ K), in the paramagnetic bcc-α phase ($T = 1.125T_c$) and in the paramagnetic bcc-δ phase ($T = 1800$ K) evaluated at experimental lattice constants. The dots correspond to the experimental data from Refs. [11,66,67] at 300 K, $1.125T_c$, and $T = 1743$ K, respectively.

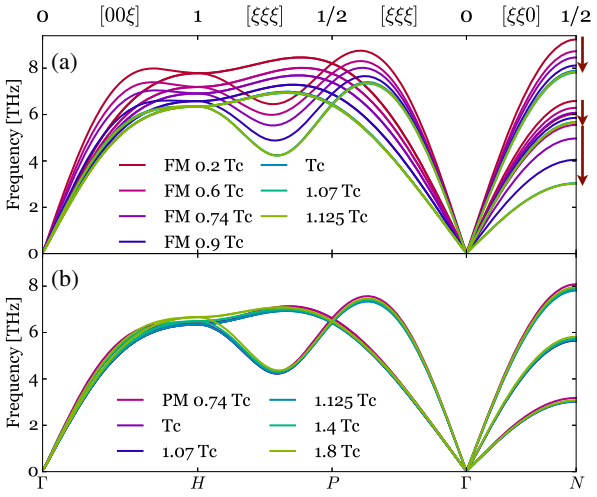

FIG. 3. (a) The calculated phonon dispersions in the bcc-α phase below and above the Curie temperature at an experimental equilibrium volume. (b) Phonons in the metastable paramagnetic bcc phase, but at a constant volume (experimental volume at $T = T_c$).

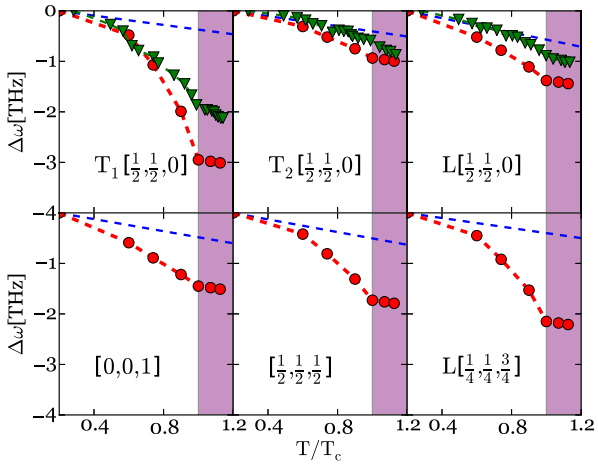

FIG. 4. The change of the phonon frequencies for representative modes with the temperature calculated by DFT + DMFT (red dots) compared to experimental data (green triangle). The dashed blue lines denote the change predicted by the quasiharmonic model: $\omega^{\mathrm{qh}}(T) = \omega^{300\,\mathrm{K}}(1-\gamma_{\mathrm{th}})(V_T - V_{300\,\mathrm{K}}/V_{300\,\mathrm{K}})$, where $\omega^{300\,\mathrm{K}}$ is the calculated value of the phonon frequency at 300 K, V_T is the experimental volume of the unit cell at temperature T, and γ_{th} is the thermal Grüneisen parameter, approximated by a constant value of 1.81, as suggested in Refs. [12,68].

was shown to similarly soften experimentally in Refs. [11,12], as well as a substantial softening in the half distance between the H and P points. The arrows on the right mark the strong temperature variation of some phonon branches. All these trends are very consistent with experiments. In Fig. 3(b), we show a phonon dispersion when the same calculation is done in a metastable paramagnetic state below T_c, where experimentally only the ferromagnetic state is stable, and also far above T_c, in which the fcc phase is thermodynamically more stable than the simulated bcc phase. In this paramagnetic calculation, we fixed the volume to remove trivial quasiharmonic effects on the phonon dispersion. We see that the phonon dispersion remains very similar up to a very high temperature.

Figure 4 shows the temperature dependence of selected phonon-branch frequencies and their comparison to the quasiharmonic approximation (blue dashed line), which takes into account only the volume expansion. We notice the inadequacy of such an approximation, while the DMFT prediction, with melting of the long-range order, is in reasonable agreement with the experiment from Ref. [12]. The experimental change is somewhat less abrupt at T_c, likely because the short-range order persists above T_c in the experiment.

On the basis of these results, we can conclude that phonon softening, discovered experimentally many years ago [11,69], is mainly due to the melting of the magnetic long-range order and is not related to the $\alpha \rightarrow \gamma$ phase transition, in contrast to what has often been assumed [11] and concluded in the previous DMFT study [17]. In our view, both the paramagnetic bcc and the fcc phase are dynamically stable at all temperatures, and their relative stability has to be determined by comparing their respective free energies.

Since our results suggest that the phonon-softening mechanism in iron is unrelated to the α-γ structural transition, we want to demonstrate that our theory correctly predicts the thermodynamic competition of the two phases (see related work in Refs. [15,70]). The martensitic α-γ transformation is usually modeled by a continuous crystallographic transition from the initial to the final phase, and in the case of a bcc-fcc transition the Bain path [71] is most often picked, which is described by a single parameter c/a with $c/a = 1$ corresponding to the bcc and $c/a = \sqrt{2}$ to the fcc phase. In Fig. 5, we show the total energy along this path, which clearly shows the double-well profile, characteristic of the first-order phase transition, that does not require softening of the phonons for the existence of the phase transition. At low temperatures ($T = 300$, 1000 K), the global minimum is at the bcc structure ($c/a = 1$), and at a high temperature ($T = 1547$ K), it is at the fcc structure ($c/a = \sqrt{2}$). Along the path, the ferromagnetic long-range order disappears in our simulation, and at that value of c/a (yellow region) the double-well curve reaches a maximum. At a high temperature ($T = 1547$ K), where the ferromagnetic long-range order disappears for all values of c/a, the total energy still keeps the double-well shape with a very small total energy difference between the bcc and fcc phases (20 meV), in contrast to the DFT prediction, which has a single minimum with both the magnetic and nonmagnetic functionals.

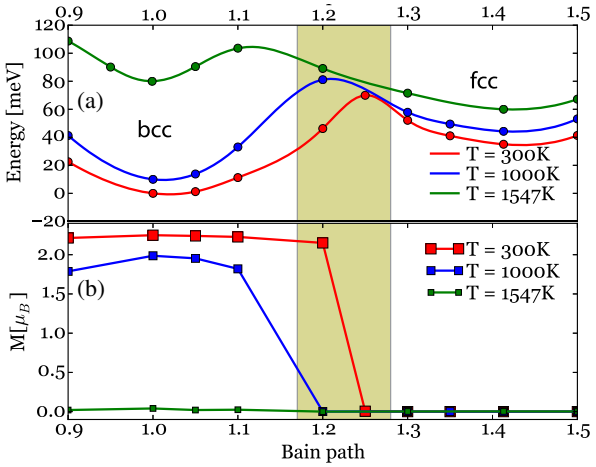

FIG. 5. (a) The total energy computed along the Bain crystallographic transition from the bcc to the fcc phase in the FM state. Note that at $T = 1547$ K the FM and PM phases are indistinguishable. (b) The ordered ferromagnetic moment along the same path.

The importance of disordered localized magnetic moments in paramagnetic phases of iron was stressed early on in the pioneering work of Grimvall [72]. This physics now emerges from a quantitative first principles method, and its implications for many physical quantities has been elucidated. We predict that the softening of the phonons in a bcc structure is not related to its first-order α to γ transition, but it is due to the melting of the long-range magnetic order. Our prediction can be checked by measuring the phonon dispersion of paramagnetic iron under an applied magnetic field, to check that long-range magnetic order in the field hardens the phonons at selected points in the Brillouin zone. We predict that the bcc structure is dynamically stable at all temperatures and is thermodynamically unstable only due to lower free energy of the fcc-γ phase at the intermediate temperatures between the α and the δ phase.

We acknowledge the support of National Science Foundation (NSF) DMR-1405303 (K. H.) and the Simons Foundation (Q. H.). T. B. was supported by the NSF (DMREF-1629260).

[1] D. J. Singh, W. E. Pickett, and H. Krakauer, Phys. Rev. B **43**, 11628 (1991).
[2] Y. Ikeda, A. Seko, A. Togo, and I. Tanaka, Phys. Rev. B **90**, 134106 (2014).
[3] F. Körmann, A. Dick, B. Grabowski, T. Hickel, and J. Neugebauer, Phys. Rev. B **85**, 125104 (2012).
[4] W. Luo, B. Johansson, O. Eriksson, S. Arapan, P. Souvatzis, M. I. Katsnelson, and R. Ahuja, Proc. Natl. Acad. Sci. U.S.A. **107**, 9962 (2010).
[5] F. Körmann, B. Grabowski, B. Dutta, T. Hickel, L. Mauger, B. Fultz, and J. Neugebauer, Phys. Rev. Lett. **113**, 165503 (2014).
[6] F. Körmann, A. Dick, B. Grabowski, B. Hallstedt, T. Hickel, and J. Neugebauer, Phys. Rev. B **78**, 033102 (2008).
[7] G. Kotliar, S. Y. Savrasov, K. Haule, V. S. Oudovenko, O. Parcollet, and C. A. Marianetti, Rev. Mod. Phys. **78**, 865 (2006).
[8] V. I. Anisimov, A. I. Poteryaev, M. A. Korotin, A. O. Anokhin, and G. Kotliar, J. Phys. Condens. Matter **9**, 7359 (1997).
[9] A. I. Lichtenstein and M. I. Katsnelson, Phys. Rev. B **57**, 6884 (1998).
[10] A. Zunger, S.-H. Wei, L. G. Ferreira, and J. E. Bernard, Phys. Rev. Lett. **65**, 353 (1990).
[11] J. Neuhaus, W. Petry, and A. Krimmel, Physica (Amsterdam) **234B**, 897 (1997).
[12] L. Mauger, M. S. Lucas, J. A. Muñoz, S. J. Tracy, M. Kresch, Y. Xiao, P. Chow, and B. Fultz, Phys. Rev. B **90**, 064303 (2014).
[13] C.-S. Lian, J.-T. Wang, and C. Chen, Phys. Rev. B **92**, 184110 (2015).
[14] A. I. Lichtenstein, M. I. Katsnelson, and G. Kotliar, Phys. Rev. Lett. **87**, 067205 (2001).
[15] I. Leonov, A. I. Poteryaev, V. I. Anisimov, and D. Vollhardt, Phys. Rev. Lett. **106**, 106405 (2011).
[16] I. Leonov, A. I. Poteryaev, V. I. Anisimov, and D. Vollhardt, Phys. Rev. B **85**, 020401 (2012).
[17] I. Leonov, A. I. Poteryaev, Y. N. Gornostyrev, A. I. Lichtenstein, M. I. Katsnelson, V. I. Anisimov, and D. Vollhardt, Sci. Rep. **4**, 5585 (2014).
[18] X. Dai, S. Y. Savrasov, G. Kotliar, A. Migliori, H. Ledbetter, and E. Abrahams, Science **300**, 953 (2003).
[19] K. Haule and T. Birol, Phys. Rev. Lett. **115**, 256402 (2015).
[20] K. Haule and G. L. Pascut, Phys. Rev. B **94**, 195146 (2016).
[21] K. Haule, C.-H. Yee, and K. Kim, Phys. Rev. B **81**, 195107 (2010).
[22] http://hauleweb.rutgers.edu/tutorials/.
[23] K. Haule, Phys. Rev. B **75**, 155113 (2007).
[24] P. Werner, A. Comanac, L. de'Medici, M. Troyer, and A. J. Millis, Phys. Rev. Lett. **97**, 076405 (2006).
[25] V. I. Anisimov and O. Gunnarsson, Phys. Rev. B **43**, 7570 (1991).
[26] K. Haule, Phys. Rev. Lett. **115**, 196403 (2015).
[27] P. Blaha, K. Schwarz, G. K. H. Madsen, D. Kvasnicka, and J. Luitz, *WIEN2K, An Augmented Plane Wave + Local Orbitals Program for Calculating Crystal Properties* (Karlheinz Schwarz, Technische Universität Wien, Austria, 2001).
[28] A. Togo and I. Tanaka, Scr. Mater. **108**, 1 (2015).
[29] Z. S. Basinski, W. Hume-Rothery, and A. L. Sutton, Proc. R. Soc. A **229**, 459 (1955).
[30] A. S. Belozerov, I. Leonov, and V. I. Anisimov, Phys. Rev. B **87**, 125138 (2013).
[31] V. I. Anisimov, A. S. Belozerov, A. I. Poteryaev, and I. Leonov, Phys. Rev. B **86**, 035152 (2012).
[32] J. Schäfer, M. Hoinkis, E. Rotenberg, P. Blaha, and R. Claessen, Phys. Rev. B **72**, 155115 (2005).
[33] See Supplemental Material at http://link.aps.org/supplemental/10.1103/PhysRevLett.120.187203 for details on our theoretical computational method and raw data for electron's self-energy, inverse quasiparticle lifetime, mass enhancement, and iron $3d$ occupancies.
[34] J. M. Luttinger and J. C. Ward, Phys. Rev. **118**, 1417 (1960).

[35] G. Baym, Phys. Rev. **127**, 1391 (1962).
[36] R. P. Feynman, Phys. Rev. **56**, 340 (1939).
[37] S. Mandal, R. E. Cohen, and K. Haule, Phys. Rev. B **89**, 220502 (2014).
[38] S. Mandal, R. E. Cohen, and K. Haule, Phys. Rev. B **90**, 060501 (2014).
[39] Z. P. Yin, K. Haule, and G. Kotliar, Nat. Phys. **10**, 845 (2014).
[40] C.-Y. Moon, H. Park, K. Haule, and J. H. Shim, Phys. Rev. B **94**, 224511 (2016).
[41] K. Ohta, R. E. Cohen, K. Hirose, K. Haule, K. Shimizu, and Y. Ohishi, Phys. Rev. Lett. **108**, 026403 (2012).
[42] M. K. Stewart, C.-H. Yee, J. Liu, M. Kareev, R. K. Smith, B. C. Chapler, M. Varela, P. J. Ryan, K. Haule, J. Chakhalian, and D. N. Basov, Phys. Rev. B **83**, 075125 (2011).
[43] K. Haule, T. Birol, and G. Kotliar, Phys. Rev. B **90**, 075136 (2014).
[44] X. Deng, A. Sternbach, K. Haule, D. N. Basov, and G. Kotliar, Phys. Rev. Lett. **113**, 246404 (2014).
[45] W. H. Brito, M. C. O. Aguiar, K. Haule, and G. Kotliar, Phys. Rev. Lett. **117**, 056402 (2016).
[46] H. C. Choi, B. I. Min, J. H. Shim, K. Haule, and G. Kotliar, Phys. Rev. Lett. **108**, 016402 (2012).
[47] H. C. Choi, K. Haule, G. Kotliar, B. I. Min, and J. H. Shim, Phys. Rev. B **88**, 125111 (2013).
[48] B. Chakrabarti, M. E. Pezzoli, G. Sordi, K. Haule, and G. Kotliar, Phys. Rev. B **89**, 125113 (2014).
[49] X. Deng, K. Haule, and G. Kotliar, Phys. Rev. Lett. **111**, 176404 (2013).
[50] J.-X. Zhu, R. C. Albers, K. Haule, G. Kotliar, and J. M. Wills, Nat. Commun. **4**, 2644 (2013).
[51] H. Zhang, K. Haule, and D. Vanderbilt, Phys. Rev. Lett. **111**, 246402 (2013).
[52] T. Birol and K. Haule, Phys. Rev. Lett. **114**, 096403 (2015).
[53] H. Zhang, K. Haule, and D. Vanderbilt, Phys. Rev. Lett. **118**, 026404 (2017).
[54] A. A. Katanin, A. I. Poteryaev, A. V. Efremov, A. O. Shorikov, S. L. Skornyakov, M. A. Korotin, and V. I. Anisimov, Phys. Rev. B **81**, 045117 (2010).
[55] M. T. Czyżyk and G. A. Sawatzky, Phys. Rev. B **49**, 14211 (1994).
[56] A. Santoni and F. J. Himpsel, Phys. Rev. B **43**, 1305 (1991).
[57] A. S. Belozerov and V. I. Anisimov, J. Phys. Condens. Matter **26**, 375601 (2014).
[58] G. K. H. Madsen and P. Novák, Europhys. Lett. **69**, 777 (2005).
[59] A. K. McMahan, R. M. Martin, and S. Satpathy, Phys. Rev. B **38**, 6650 (1988).
[60] M. S. Hybertsen, M. Schlüter, and N. E. Christensen, Phys. Rev. B **39**, 9028 (1989).
[61] F. Aryasetiawan, M. Imada, A. Georges, G. Kotliar, S. Biermann, and A. I. Lichtenstein, Phys. Rev. B **70**, 195104 (2004).
[62] F. Aryasetiawan, K. Karlsson, O. Jepsen, and U. Schönberger, Phys. Rev. B **74**, 125106 (2006).
[63] T. Miyake, F. Aryasetiawan, and M. Imada, Phys. Rev. B **80**, 155134 (2009).
[64] http://stokes.byu.edu/iso/smodes.php.
[65] J. Sánchez-Barriga, J. Fink, V. Boni, I. Di Marco, J. Braun, J. Minár, A. Varykhalov, O. Rader, V. Bellini, F. Manghi, H. Ebert, M. I. Katsnelson, A. I. Lichtenstein, O. Eriksson, W. Eberhardt, and H. A. Dürr, Phys. Rev. Lett. **103**, 267203 (2009).
[66] V. J. Minkiewicz, G. Shirane, and R. Nathans, Phys. Rev. **162**, 528 (1967).
[67] J. Neuhaus, M. Leitner, K. Nicolaus, W. Petry, B. Hennion, and A. Hiess, Phys. Rev. B **89**, 184302 (2014).
[68] O. L. Anderson, Geophys. J. Int. **143**, 279 (2000).
[69] S. K. Satija, R. P. Comès, and G. Shirane, Phys. Rev. B **32**, 3309 (1985).
[70] A. A. Katanin, A. S. Belozerov, and V. I. Anisimov, Phys. Rev. B **94**, 161117 (2016).
[71] S. V. Okatov, A. R. Kuznetsov, Y. N. Gornostyrev, V. N. Urtsev, and M. I. Katsnelson, Phys. Rev. B **79**, 094111 (2009).
[72] G. Grimvall, Phys. Scr. **13**, 59 (1976).